electronics

Article

Study of the Within-Batch TID Response Variability on Silicon-Based VDMOS Devices

Xiao Li [1,2,3], Jiangwei Cui [1,2,3,*], Qiwen Zheng [1,2,3,*], Pengwei Li [4], Xu Cui [1,2,3], Yudong Li [1,2,3] and Qi Guo [1,2,3]

1 Key Laboratory of Functional Materials and Devices for Special Environments, Xinjiang Technical Institute of Physics and Chemistry, Chinese Academy of Sciences, Urumqi 830011, China
2 Xinjiang Key Laboratory of Electronic Information Material and Device, Xinjiang Technical Institute of Physics and Chemistry, Chinese Academy of Sciences, Urumqi 830011, China
3 University of Chinese Academy of Sciences, Beijing 100049, China
4 China Academy of Space Technology, Beijing 100049, China
* Correspondence: cuijw@ms.xjb.ac.cn (J.C.); qwzheng@ms.xjb.ac.cn (Q.Z.)

Abstract: Silicon-based vertical double-diffused MOSFET (VDMOS) devices are important components of the power system of spacecraft. However, VDMOS is sensitive to the total ionizing dose (TID) effect and may have TID response variability. The within-batch TID response variability on silicon-based VDMOS devices is studied by the ^{60}Co gamma-ray irradiation experiment in this paper. The variations in device parameters after irradiation is obtained, and the damage mechanism is revealed. Experimental results show that the standard deviations of threshold voltage, subthreshold swing, output capacitance, and diode forward voltage increase, while the standard deviation of maximum transconductance decreases after irradiation. The standard deviation of on-state resistance is basically unchanged before and after irradiation. By separating the trapped charges generated by TID irradiation, it is found that the deviation of the oxide trapped charges and the interface traps increase with the increase in the total dose. The reasons for the variation in device parameters after irradiation are revealed by establishing the relationship between the trapped charges and the electrical parameters before and after irradiation.

Keywords: VDMOS; total ionizing dose (TID); variability; oxide trapped charges; interface traps

Citation: Li, X.; Cui, J.; Zheng, Q.; Li, P.; Cui, X.; Li, Y.; Guo, Q. Study of the Within-Batch TID Response Variability on Silicon-Based VDMOS Devices. *Electronics* **2023**, *12*, 1403. https://doi.org/10.3390/electronics12061403

Academic Editor: Adel M. Sharaf

Received: 13 January 2023
Revised: 8 March 2023
Accepted: 10 March 2023
Published: 15 March 2023

Copyright: © 2023 by the authors. Licensee MDPI, Basel, Switzerland. This article is an open access article distributed under the terms and conditions of the Creative Commons Attribution (CC BY) license (https://creativecommons.org/licenses/by/4.0/).

1. Introduction

Silicon-based vertical double-diffused MOSFET (VDMOS) devices are widely used in the power system of spacecraft due to the high input impedance, large current gain, excellent noise margin, and small conduction loss, as well as a negative temperature coefficient and no secondary breakdown effect [1,2]. However, VDMOS is sensitive to the total ionizing dose (TID) effect since there is a parasitic NPN transistor in the VDMOS structure [3]. Moreover, process variation in VDMOS manufacturing occurs with different temperature distributions, impurity diffusion, and injection. The TID response is sensitive to process variations, as evidenced by the different TID responses of devices produced from the same wafer (within-wafer) or devices produced from the same batch (within-batch).

The TID response variability has been studied in previous works. Within-wafer TID response variability of NMOSFET and PMOSFET was measured by Hu et al. and Gerardin et al. [4,5]. They attributed the within-wafer TID response variability to the process variation in shallow trench isolation (STI) and random doping. The TID response variability of 25 nm single-level cell non-volatile memory device (NAND) flash memories from two different lots was studied by Bagatin et al. [6]. The statistical parameters such as mean value, standard deviation, and shapes of the error distributions were studied. Part-to-part and lot-to-lot variability of TID response in bipolar linear devices was studied by Guillermin et al. [7]. The three-sigma method and one-sided tolerance limit method were commonly used to take the variability into account. Within-wafer TID response variability

on the buried oxide (BOX) layer of silicon-on-insulator (SOI) technology was investigated by Zheng et al. [8,9]. The larger standard deviation of threshold voltage and off-state leakage distribution for irradiated devices than un-irradiated devices were observed. They attributed it to the evolution of net trapped charges induced by TID in BOX affecting by positively charged silicon nanoclusters introduced by silicon ion implantation. The device variability induced by the TID effects was investigated by Ma et al. in commercial 16 nm bulk nFinFETs with a small number of samples [10]. It was found that transistors characterized by higher drain currents exhibit the worst TID degradation. They attributed this phenomenon to the impact of random dopant fluctuations on the TID effects and/or to variations in the hydrogen concentration responsible for the TID-induced interface traps. The above studies confirmed the fluctuation of the TID response of the devices in the wafer, as well as the variability of the radiation damage of device modules from different batches and within-batch. There have been studies on the TID effect of VDMOS [11–15]. However, to our best knowledge, there is no report on the within-batch TID response variability on silicon-based VDMOS devices.

Within-batch TID response variability on silicon-based VDMOS devices is investigated by irradiation experiment in this paper. The variability of threshold voltage, subthreshold swing, maximum transconductance, output capacitance, diode forward voltage, and on-state resistance before and after irradiation is analyzed. The reasons for the variation in device parameters under irradiation are revealed by analyzing the trapped charge induced by irradiation.

2. Experiment Details

The devices under test (DUT) are N-channel enhanced VDMOS within the same batch. When the device is turned on, the maximum drain current is 120A. The maximum gate-source voltage is 20 V. The device has three terminals, gate, drain, and source. The device is packaged with TO247. The numbers of DUT are from 1 to 68. The experiments were conducted by ^{60}Co gamma-ray at room temperature in the Xinjiang Technical Institute of Physics and Chemistry, Chinese Academy of Sciences. The dose rate was 50.24 rad(Si)/s and the dose levels were 5 krad(Si), 10 krad(Si), 15 krad(Si), 20 krad(Si), and 25 krad(Si). It was found that the ON bias condition ($V_{DS} = 0$ V, $V_{GS} = 20$ V) can induce greater radiation damage than other bias conditions. All devices were kept ON bias condition during the irradiation process.

The transfer characteristic curves $(I_{DS} - V_{GS})$ of the devices were measured by Keysight B1500A semiconductor parameter analyzer at room temperature, while the drain voltage was set to 0.1 V, the gate voltage swept between −0.5 V and 5 V, and the source was grounded. The threshold voltage (V_{TH}) of the device was extracted by the constant current method. V_{TH} is equal to the gate-source voltage (V_{GS}) when the drain current is equal to 250 μA. The subthreshold swing (SS) of the device was calculated by $SS = \frac{\mathrm{d}V_{GS}}{\mathrm{d}(\log I_{DS})}$. The transconductance was calculated by $G_M = \frac{dI_{DS}}{dV_{GS}}$. G_{MMAX} is the max transconductance. The output capacitance (C_{OSS}) was measured, while the frequency was 1.0 MHz, the gate-source voltage was 0 V, and the drain-source voltage was 25 V. The on-state resistance $\left(R_{DS(ON)}\right)$ and diode forward voltage (V_{SD}) were measured by BC3193 Semiconductor Discrete Device Test System at room temperature. The specific parameters and test conditions are shown in Table 1.

Table 1. Test parameters of silicon-based VDMOS.

Test Equipment	Test Parameter	Test Conditions
B1500A	V_{TH}	$V_{DS} = V_{GS}, I_{DS} = 250$ µA
B1500A	SS	$V_{DS} = 0.1$ V, $I_{DS} - V_{GS}$ Curve
B1500A	G_{MMAX}	$V_{DS} = 0.1$ V, $I_{DS} - V_{GS}$ Curve
B1500A	C_{OSS}	$V_{DS} = 25$ V, $V_{GS} = 0$ V, $f = 1$ MHz
BC3193	V_{SD}	$V_{GS} = 0$ V, $I_S = 75$ A
BC3193	$R_{DS(ON)}$	$V_{GS} = 10$ V, $I_D = 75$ A

3. Experimental Results

The $I_{DS} - V_{GS}$ curves of 68 devices before and after TID irradiation are shown in Figure 1. It can be seen that the $I_{DS} - V_{GS}$ curves of the devices shift negatively as the dose increases. The variability between devices increases after irradiation.

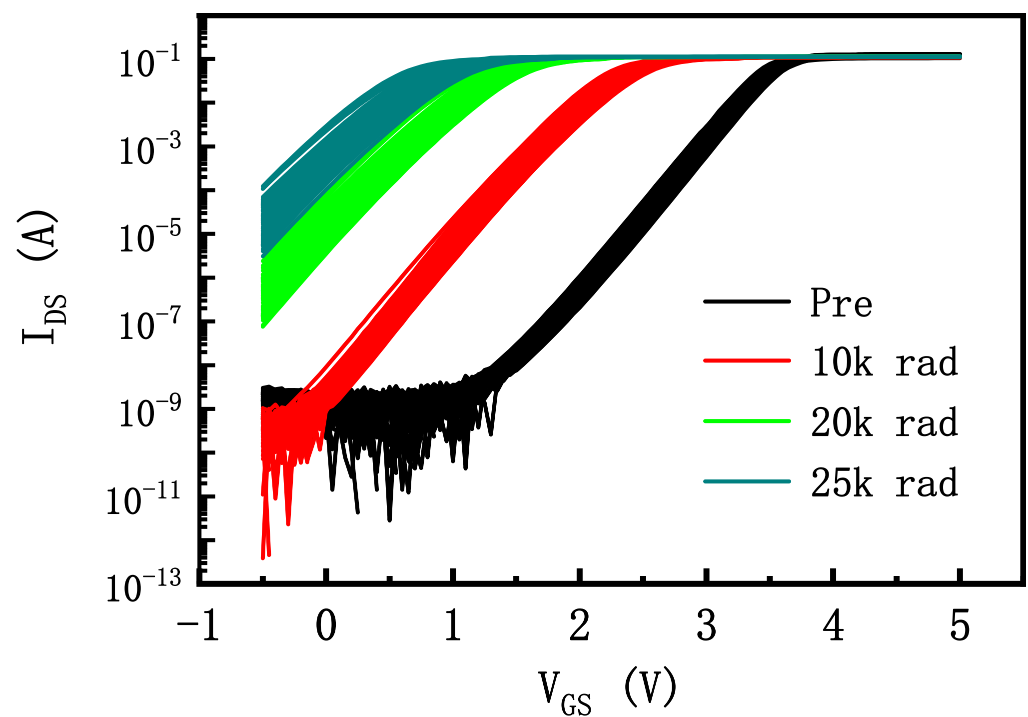

Figure 1. The shift of transfer characteristic curves of VDMOS devices before and after irradiation.

The variation in threshold voltage, subthreshold swing, and maximum transconductance extracted by the $I_{DS} - V_{GS}$ curves after irradiation is shown in Figure 2a, Figure 2b, and Figure 2c respectively. The mean value and standard deviation (σ) of the electrical parameters are calculated. With the increase in the total dose, the standard deviation of threshold voltage and subthreshold swing increase, while the standard deviation of maximum transconductance decreases. The experiment results verify the within-batch TID response variability on the VDMOS device since standard deviation measures the dispersion of a dataset relative to its mean value [8].

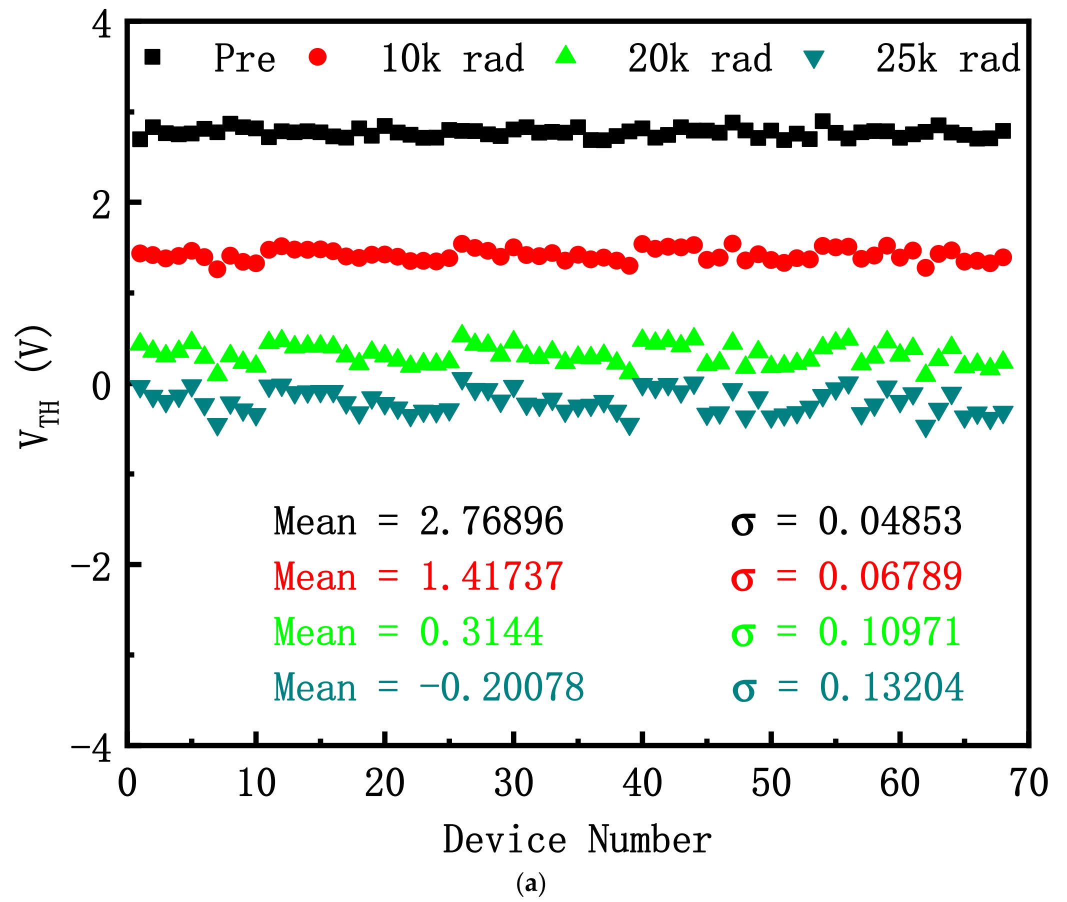

(a)

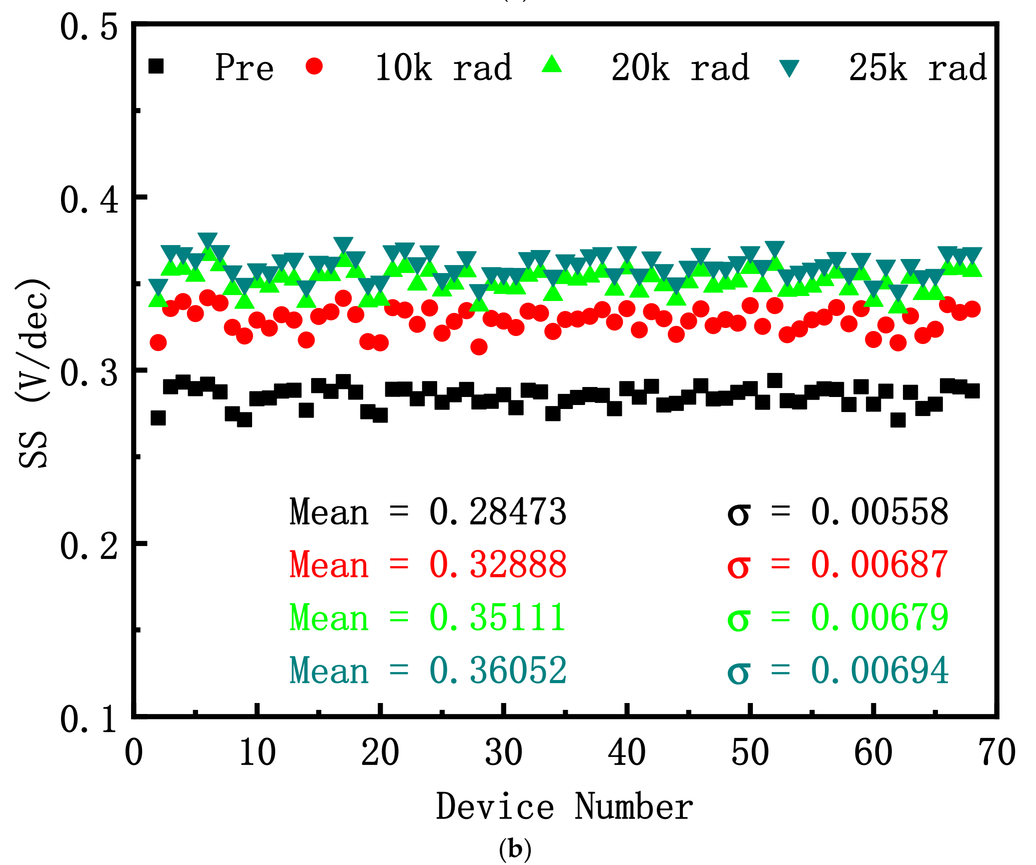

(b)

Figure 2. *Cont.*

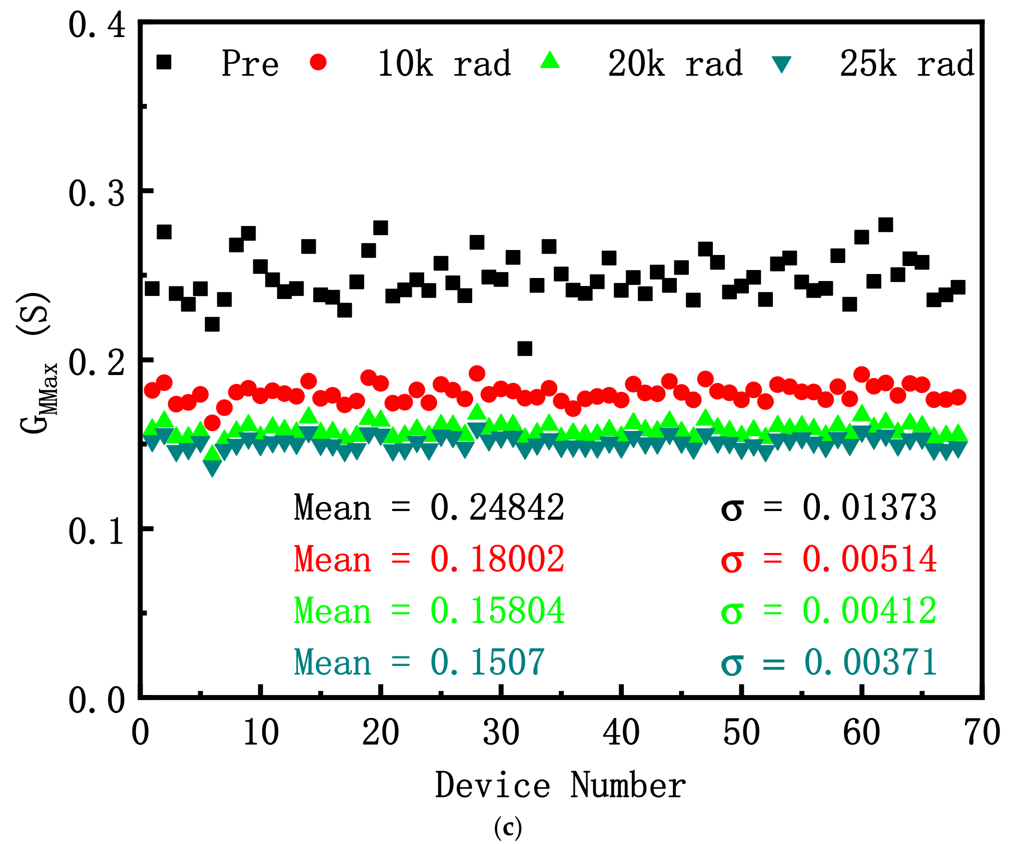

(**c**)

Figure 2. The variation in (**a**) V_{TH}, (**b**) SS, and (**c**) G_{MMAX} of the devices before and after irradiation.

The variation in output capacitance after irradiation is shown in Figure 3. The mean value and standard deviation of the electrical parameters increase after irradiation, which indicates that output capacitance variability also increases after irradiation.

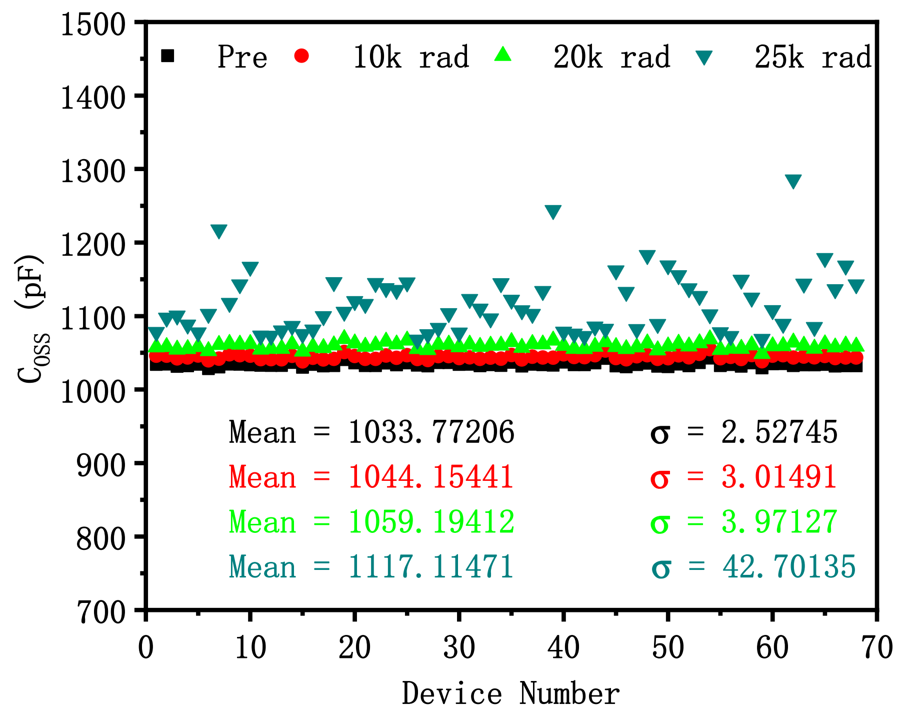

Figure 3. The variation in C_{OSS} of the devices before and after irradiation.

The variation in diode forward voltage and the on-state resistance after irradiation is shown in Figures 4 and 5, respectively. It can be seen that the variability of diode forward voltage increases as the total dose increases. The variability of on-state resistance is basically unchanged before and after irradiation.

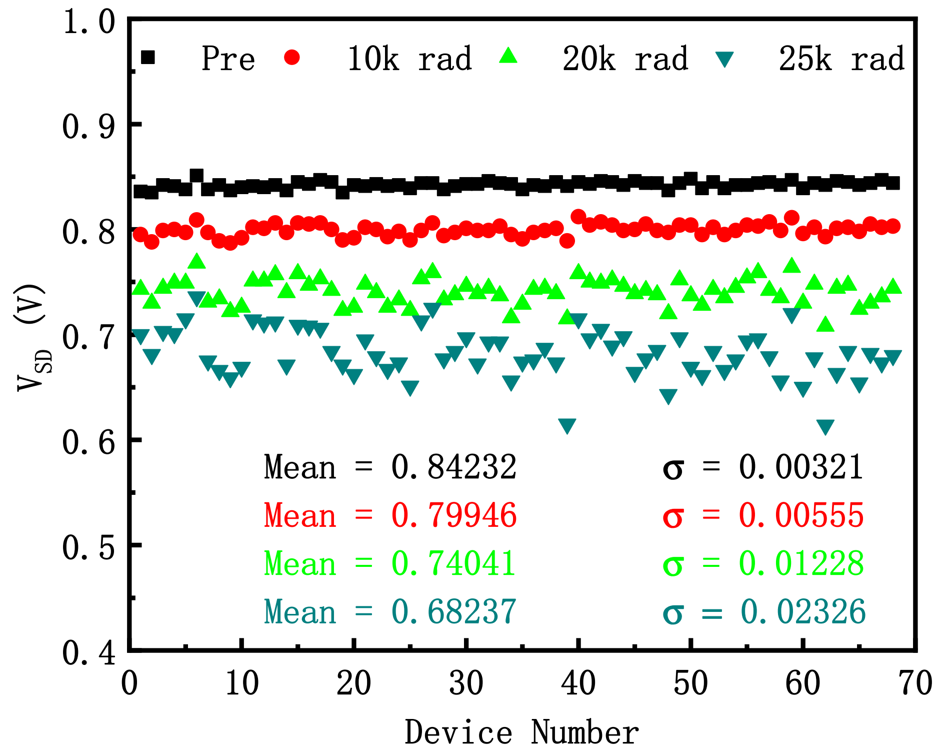

Figure 4. The variation in V_{SD} of the devices before and after irradiation.

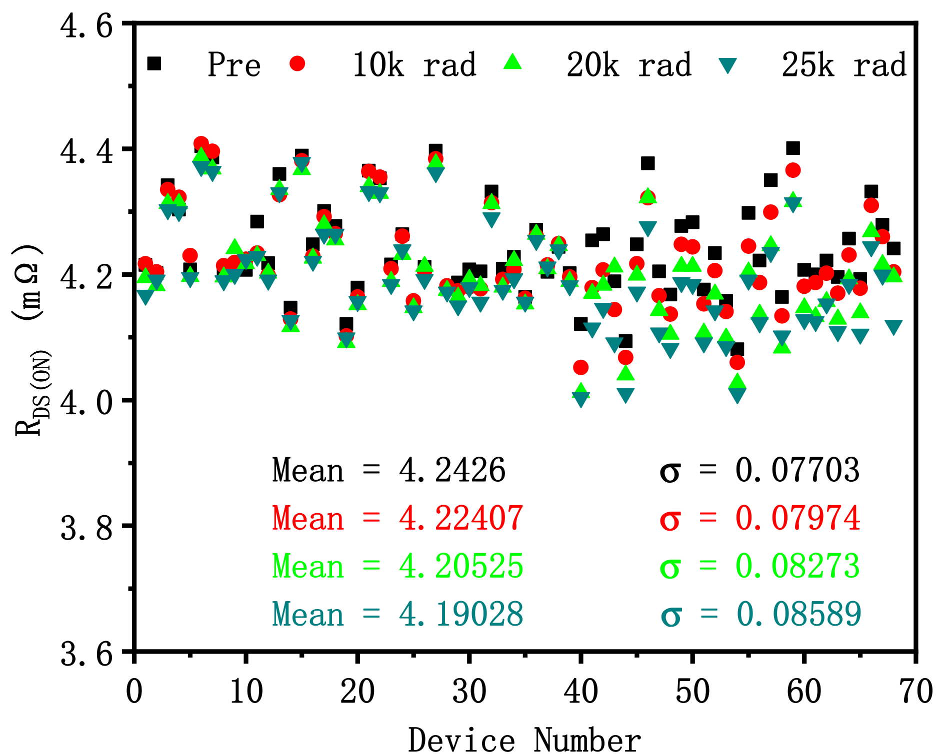

Figure 5. The variation in $R_{DS(ON)}$ of the devices before and after irradiation.

It can be seen from the above results that there is within-batch TID response variability of VDMOS devices in this paper. The changes in parameter variability after irradiation are listed in Table 2.

Table 2. The variation in test parameters of the devices after irradiation.

Test Parameter	Standard Deviation
V_{TH}	Increase
SS	Increase
G_{MMAX}	Decrease
C_{OSS}	Increase
V_{SD}	Increase
$R_{DS(ON)}$	Not Obvious

4. Discussion

For MOS devices, the initial electron–hole pairs generated by TID irradiation will eventually affect the electrical parameters of devices through a series of evolution. Four physical processes illustrate the evolution of electron–hole pairs generated by ionizing radiation at the interface of the SiO_2 gate and Si substrate, as shown in Figure 6 [16].

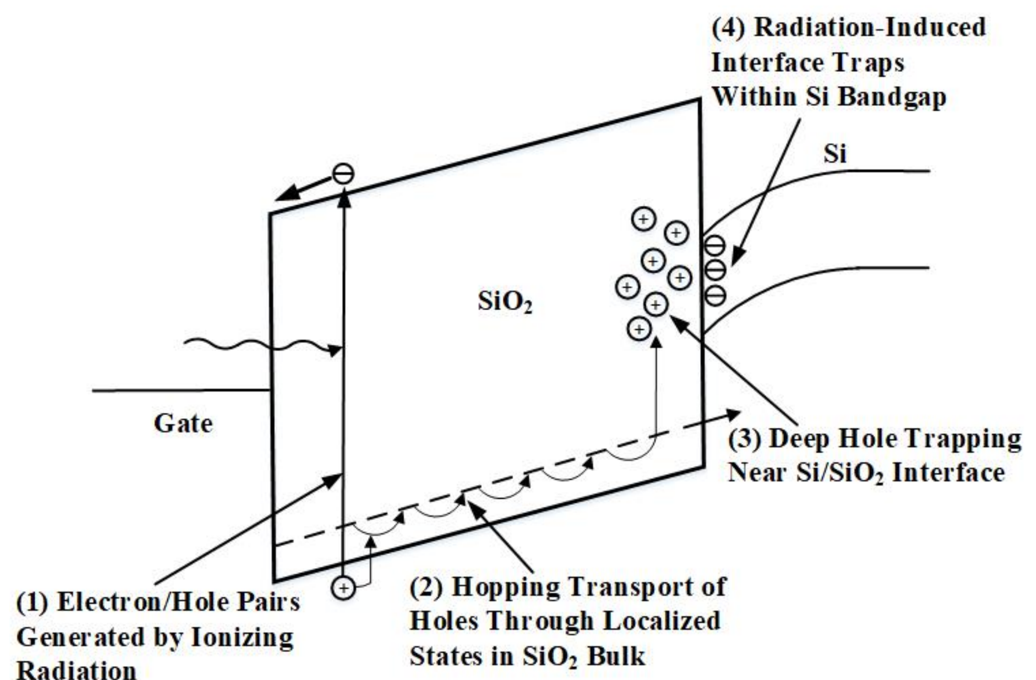

Figure 6. Band diagram of a MOS capacitor with a positive gate bias. Illustrated are the main processes for radiation-induced charge generation [16].

The specific process is as follows [16–19]:

1. The ionization of radiation particles in SiO_2 produces electron–hole pairs, the number of which is related to the ionization dose.
2. When the positive bias is applied to the gate, the drift motion of the electron–hole pairs in the oxide layer is the most significant. The electrons are removed by a fast drift (ps magnitude) towards the anodic ohmic contact, and the holes are relatively slow (s magnitude) to the cathodic ohmic contact.
3. In the drift process, some holes are captured to form the trap center. In the shallow-level trap center located in the gap of SiO_2, about 1 eV is distributed in the whole SiO_2 body. The holes can be transported in a jump mode. The center of the deep-level trap

with more than 3 eV in the gap of SiO_2 is mainly distributed near the SiO_2-Si interface, which is the relatively stable positive charge (N_{ot}) trapped by the oxide layer.

4. In the transition layer of the SiO_2-Si interface, the holes captured by the oxide layer are exchanged with the electrons in the substrate Si through the tunneling effect and finally captured by the defects at the interface to form the interface traps (N_{it}).
5. Therefore, the main reason for the variation in device parameters after irradiation is that the ionizing radiation destroys the energy band equilibrium, generates electron–hole pairs, and forms oxide-trapped charges and interface traps. The oxide layer is the most sensitive part to TID radiation in the MOS system [19].

A technique for separating the density of oxide-trapped charges (N_{ot}) and the density of interface traps (N_{it}) in MOS transistors through $I - V$ curves is proposed by McWhorter and Winokur [20,21]. In order to reveal the mechanism of the TID variability response of devices within-batch, the N_{ot} and N_{it} of devices used in this paper were extracted, as shown in Figure 7. The variability of N_{ot} and N_{it} of the devices increases as the total dose increases. It shows that the trapped charges induced by total dose irradiation have fluctuation, which causes the variability of relevant sensitive electrical parameters. The density of N_{ot} is much higher than the density of N_{it}, while N_{ot} is about $10^{12}/cm^2$, and N_{it} is about $10^{11}/cm^2$ at 25 krad(Si).

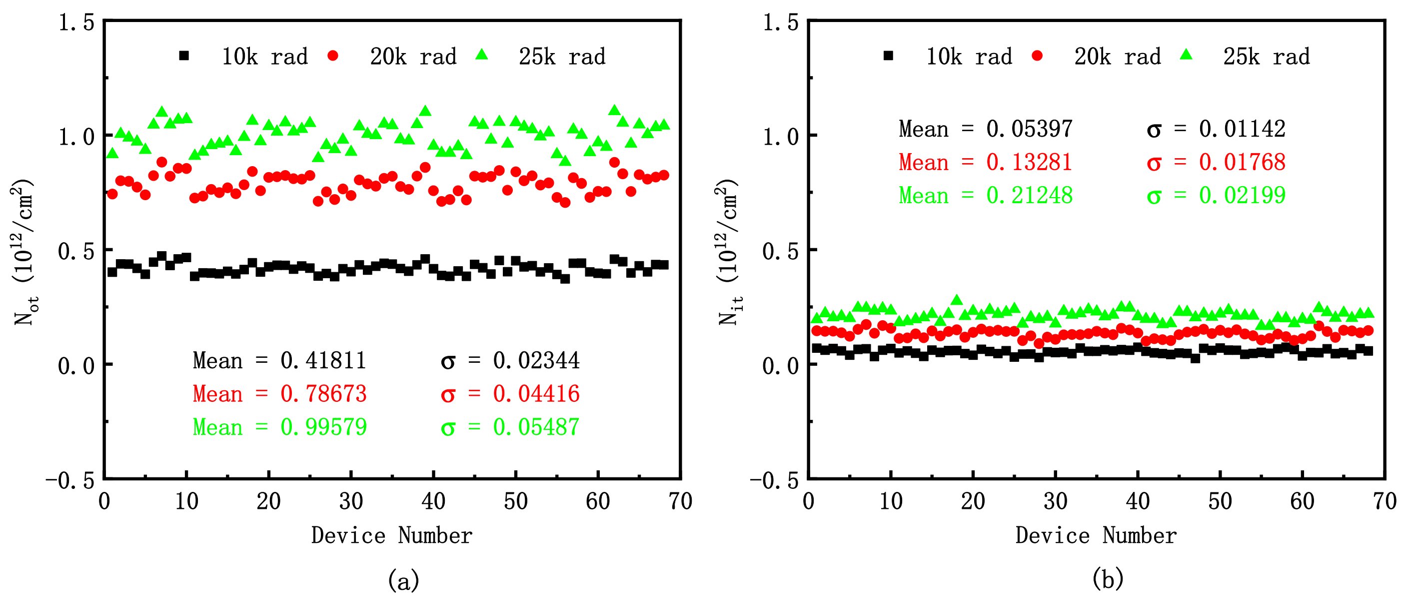

Figure 7. The variation in (**a**) oxide trapped charge (N_{ot}) density, (**b**) interface trap charge (N_{it}) density of the devices after irradiation.

Figure 8 shows the relation between the shift of threshold voltage (ΔV_{TH}) and the trapped charges ($|N_{ot}| - |N_{it}|$) of the within-batch devices after irradiation. As seen from the fit curve in Figure 8, the ΔV_{TH} and the $|N_{ot}| - |N_{it}|$ present the linear growth trend. For NMOSFET, the oxide-trapped charges cause a negative shift of the threshold voltage, while the interface traps cause a positive shift of the threshold voltage [3,19]. The calculation formula between ΔV_{TH} and trapped charges is [13,22–24]:

$$\Delta V_{TH} = -\frac{q|N_{ot}| - |N_{it}|}{C_{ox}} \quad (1)$$

where q (amount of charge) and C_{ox} (the gate oxide capacitance per unit area) are constant values. Since the density of N_{ot} is much higher than the density of N_{it}, the variability of the threshold voltage is mainly affected by the variability of N_{ot}.

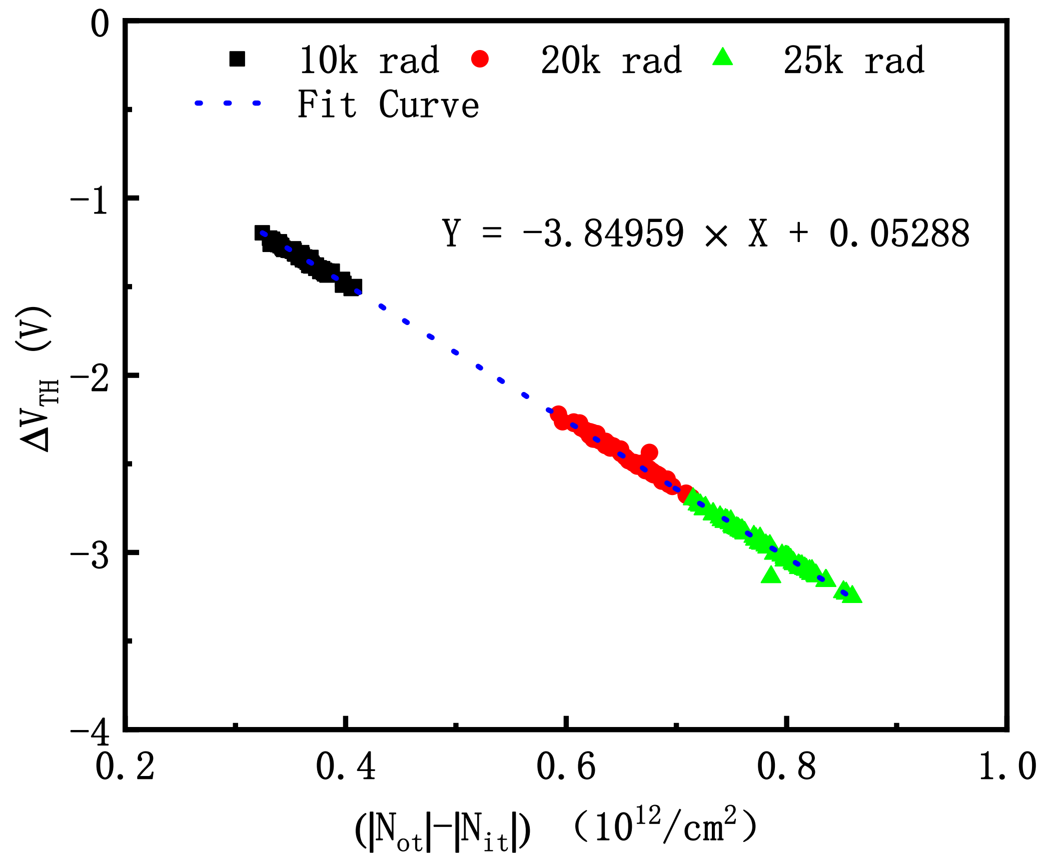

Figure 8. Relation between the shift of threshold voltage (ΔV_{TH}) and the trapped charges ($|N_{ot}| - |N_{it}|$) of the devices after irradiation.

V_{SD} is the forward voltage of the diode between the source and the drain. The threshold voltage reduces significantly or even becomes negative after irradiation, resulting in a conductive channel. Additionally, V_{SD} is across the source, channel, and drain [18,25]. V_{SD} is mainly affected by the threshold voltage, so the trend of within-batch variability is the same as the threshold voltage after irradiation.

Subthreshold swing and maximum transconductance are mainly affected by radiation-induced interface traps [26–29]. Interface traps are formed by TID irradiation at the interface between the device gate dielectric and the silicon substrate. The increase in the interface traps degrades the subthreshold swing of the devices [26]. The formula for SS is [21,30]:

$$SS = (\text{In}10)\left(\frac{KT}{q}\right)\left(\frac{C_{ox} + C_D + C_{it}}{C_{ox}}\right) \tag{2}$$

$$C_{it} = q^2 D_{it} = \beta N_{it} \tag{3}$$

where K is the Boltzmann constant, T is the absolute temperature, C_D is the depletion layer capacitance, C_{it} is the interface traps capacitance, D_{it} is the interface traps density, and β is the correlation coefficient. Therefore, the within-batch variability of subthreshold swing increases after irradiation.

The variability of maximum transconductance is negatively correlated with the interface traps variability, while the variability trends of maximum transconductance and subthreshold swing are opposite. The formula for G_{MMAX} and N_{it} is [2,31,32]:

$$G_{MMAX} = G_{M0}\frac{1}{1 + \alpha N_{it}} \tag{4}$$

where G_{M0} and G_{MMAX} are the maximum transconductance values before and after irradiation, and α is the process fluctuation constants of the devices.

Figure 9 shows the relation between the shift of output capacitance (ΔC_{oss}) and N_{ot} of the within-batch devices after irradiation. As seen from the fit curve in Figure 9, the variation in ΔC_{OSS} and the N_{ot} presents the exponential growth trend. Therefore, the variability of output capacitance increases sharply at 25 krad(Si) in Figure 3. The output capacitance is equal to the sum of the drain-source capacitance and the gate-drain capacitance. The drain-source capacitance is the junction capacitance, which is not changed by the increase in radiation dose [19,33]. Therefore, the variation in output capacitance induced by TID is mainly affected by the gate-drain capacitance, which is a function of oxide capacitance, reverse capacitance, and depleted capacitance [33,34]. The output capacitance is sensitive to N_{ot}, so as to characterize the correlation between C_{OSS} and N_{ot}.

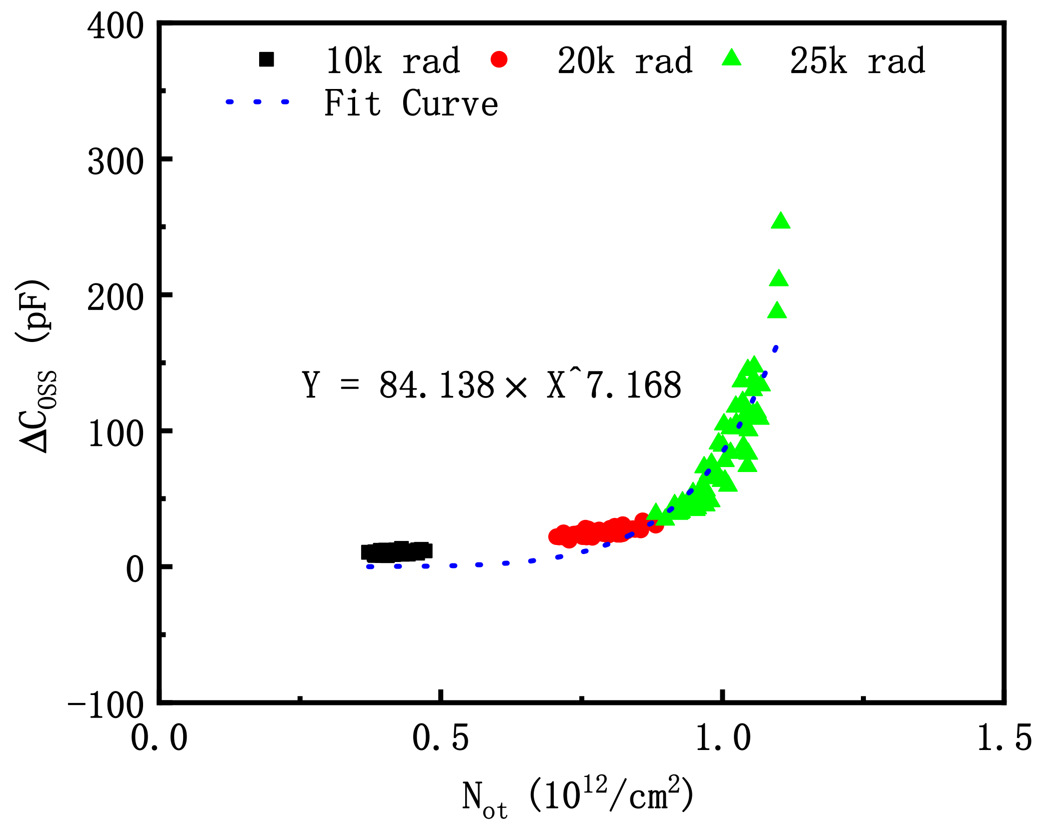

Figure 9. Relation between the shift of output capacitance (ΔC_{OSS}) and the oxide-trapped charge (N_{ot}) of the devices after irradiation.

The on-state resistance is regulated by the channel reverse voltage ($V_{GS} - V_{TH}$), which is closely related to the N_{ot} [25,35]. Because V_{GS} is much larger than the variation in V_{TH}, the variability of oxide trapped charges have no obvious effect on the variability of $R_{DS(ON)}$.

In general, the accumulation of trapped charges after irradiation magnifies the process differences of devices in the same batch and leads to differential variability in threshold voltage, subthreshold swing, maximum transconductance, output capacitance, and diode forward voltage. The correlations between the variations in electrical parameters and the trapped charges after irradiation are shown in Table 3. However, the variation in electrical parameters of devices in the same batch is a disadvantage to the stability and reliability of the spacecraft, which would lead to thermal failure, an unreasonable dead zone, or gate resonance problems in the circuit module. The differences in threshold voltage and output capacitance must be considered in the circuit design of space equipment, and the variability of on-state resistance in the same batch can be tolerated after irradiation.

Table 3. Correlation between the variation in electrical parameters and the trapped charges generated by irradiation.

Parameter	Elements	Major Impacts
V_{TH}	The oxide-trapped charges and the interface traps work together	Positively correlated with N_{ot}
SS	$SS = (\text{In}10)\left(\frac{KT}{q}\right)\left(\frac{C_{ox}+C_D+\beta N_{it}}{C_{ox}}\right)$	Positively correlated with N_{it}
G_{MMAX}	$G_M = G_{M0}\frac{1}{1+\alpha N_{it}}$, Contrary to the trend of SS changes	Negatively correlated with N_{it}
C_{OSS}	It is related to the increase in the number of charges in the space charge region and the decrease in the width of the depletion layer	Exponential Relationship with N_{ot}
V_{SD}	After irradiation, a conductive channel is formed, and the changing trend is the same as the threshold voltage	Positively correlated with N_{ot}
$R_{DS(ON)}$	Regulation of channel reverse voltage (V_{GS}-V_{TH})	No Obvious

5. Conclusions

Silicon-based VDMOS devices are important components of the power system of spacecraft. However, the VDMOS is sensitive to the TID effect. Moreover, the TID response is sensitive to process variation, behaving as within-batch TID response variability. The within-batch TID response variability on silicon-based VDMOS devices is investigated by the ^{60}Co gamma-ray irradiation experiment in this paper. Experimental results show that with the increase in total dose, the variability of the within-batch devices parameters changes. The variability of threshold voltage, subthreshold swing, output capacitance, and diode forward voltage increases after irradiation. Furthermore, the variability of maximum transconductance decreases after irradiation, and the variability of on-state resistance is basically unchanged before and after irradiation. By extracting N_{ot} and N_{it} induced by TID irradiation in the devices, the relationship between the parameters variation and trapped charges are established, and the reasons for within-batch TID response variability are clarified.

Among them, it should be noted that the variability of threshold voltage and output capacitance within-batch shows different functional trends with the increase in radiation dose. The differences in threshold voltage and output capacitance must be considered in some new spacecraft. The new generation of spacecraft requires higher reliability and better performance of electronic devices. The electrical parameter margins are very small in some circuits. Considering the variability of electrical parameters between the same batch of devices caused by TID can reduce the loss and protect the circuit more accurately. The variability of on-state resistance in the same batch can be tolerated after irradiation in the circuit design of space equipment. This study provides a foundation for the establishment of scientific and reasonable TID effect evaluation and screening methods on the within-batch devices so as to ensure the stability and reliability of the power system of spacecraft.

Author Contributions: Conceptualization, J.C. and Q.Z.; methodology, writing—original draft preparation X.L.; writing—review and editing, J.C.; supervision, Y.L. and Q.G.; data curation, X.C.; formal analysis, P.L. All authors have read and agreed to the published version of the manuscript.

Funding: This work was supported in part by the Youth Innovation Promotion Association CAS (2020430), the West Light Foundation of the Chinese Academy of Science under Grant No. 2019-XBQNXZ-A-003, the National Natural Science Foundation of China under Grant 12275352, and the project under Grant No. 2022D14003.

Data Availability Statement: The data presented in this study are available on reasonable request from the corresponding authors.

Conflicts of Interest: The authors declare no conflict of interest.

References

1. Grant, D.A.; Gowar, J. *Power MOSFETS: Theory and Applications*, 1st ed.; John Wiley & Sons, Incorporated: New York, NY, USA, 1989; pp. 17–21.
2. Singh, G.; Galloway, K.F.; Russell, T.J. Radiation-Induced Interface Traps in Power Mosfets. *IEEE Trans. Nucl. Sci.* **1986**, *33*, 1454–1459. [CrossRef]
3. Wang, H. Research on the Radiation Effects of VDMOS Power Devices in Space Instruments. Master's Thesis, National University of Defense Technology, Changsha, China, 2017.
4. Hu, Z.; Liu, Z.; Shao, H.; Zhang, Z.; Ning, B.; Chen, M.; Bi, D.; Zou, S. Impact of within-wafer process variability on radiation response. *Microelectron. J.* **2011**, *42*, 883–888. [CrossRef]
5. Gerardin, S.; Bagatin, M.; Cornale, D.; Ding, L.; Mattiazzo, S.; Paccagnella, A.; Faccio, F.; Michelis, S. Enhancement of Transistor-to-Transistor Variability Due to Total Dose Effects in 65-nm MOSFETs. *IEEE Trans. Nucl. Sci.* **2015**, *62*, 2398–2403. [CrossRef]
6. Bagatin, M.; Gerardin, S.; Ferrarese, F.; Paccagnella, A.; Ferlet-Cavrois, V.; Costantino, A.; Muschitiello, M.; Visconti, A.; Wang, P.X. Sample-to-Sample Variability and Bit Errors Induced by Total Dose in Advanced NAND Flash Memories. *IEEE Trans. Nucl. Sci.* **2014**, *61*, 2889–2895. [CrossRef]
7. Guillermin, J.; Sukhaseum, N.; Varotsou, A.; Privat, A.; Garcia, P.; Vaillé, M.; Thomas, J.C.; Chatry, N.; Poivey, C. Part-to-part and lot-to-lot variability study of TID effects in bipolar linear devices. In Proceedings of the 2016 16th European Conference on Radiation and Its Effects on Components and Systems (RADECS), Bremen, Germany, 19–23 September 2016; pp. 1–8.
8. Zheng, Q.; Cui, J.; Yu, X.; Li, Y.; Lu, W.; He, C.; Guo, Q. Measurement and Evaluation of the Within-Wafer TID Response Variability on BOX Layer of SOI Technology. *IEEE Trans. Nucl. Sci.* **2021**, *68*, 2516–2523. [CrossRef]
9. Zheng, Q.; Cui, J.; Yu, X.; Li, Y.; Lu, W.; He, C.; Guo, Q. Impact of TID on Within-Wafer Variability of Radiation-Hardened SOI Wafers. *IEEE Trans. Nucl. Sci.* **2021**, *68*, 1423–1429. [CrossRef]
10. Ma, T.; Bonaldo, S.; Mattiazzo, S.; Baschirotto, A.; Enz, C.; Paccagnella, A.; Gerardin, S. Increased Device Variability Induced by Total Ionizing Dose in 16-nm Bulk nFinFETs. *IEEE Trans. Nucl. Sci.* **2022**, *69*, 1437–1443. [CrossRef]
11. Mo, J.J.; Chen, H.; Wang, L.P.; Yu, F.X. Total Ionizing Dose Effect and Single Event Burnout of VDMOS with Different Inter Layer Dielectric and Passivation. *J. Electron. Test.-Theory Appl.* **2017**, *33*, 255–259. [CrossRef]
12. Li, X.; Jia, Y.; Zhou, X.; Zhao, Y.; Tang, Y.; Li, Y.; Liu, G.; Jia, G. Degradation of Radiation-Hardened Vertical Double-Diffused Metal-Oxide-Semiconductor Field-Effect Transistor During Gamma Ray Irradiation Performed After Heavy Ion Striking. *IEEE Electron Device Lett.* **2020**, *41*, 216–219. [CrossRef]
13. Wang, R.; Li, Z.; Qiao, M.; Zhou, X.; Wang, T.; Zhang, B. Total Ionizing Dose Effects in 30-V Split-Gate Trench VDMOS. *IEEE Trans. Nucl. Sci.* **2020**, *67*, 2009–2014. [CrossRef]
14. Sun, Y.; Wang, T.; Liu, Z.; Xu, J. Investigation of irradiation effects and model parameter extraction for VDMOS field effect transistor exposed to gamma rays. *Radiat. Phys. Chem.* **2021**, *185*, 109478. [CrossRef]
15. Qin, Z.; Yang, J.; Li, X. Displacement damage on P-channel VDMOS caused by different energy protons. *Nucl. Instrum. Methods Phys. Res. Sect. B* **2019**, *461*, 232–236. [CrossRef]
16. Schwank, J.R.; Shaneyfelt, M.R.; Fleetwood, D.M.; Felix, J.A.; Dodd, P.E.; Paillet, P.; Ferlet-Cavrois, V. Radiation Effects in MOS Oxides. *IEEE Trans. Nucl. Sci.* **2008**, *55*, 1833–1853. [CrossRef]
17. Han, Z.; Zhao, Y. *Introduction to Radiation Hardened Integrated Circuit*, 1st ed.; Tsinghua University Press: Beijing, China, 2011; pp. 13–14.
18. Liu, W. *Radiation Effects and Reinforcement Techniques of Silicon Semiconductor Devices*, 1st ed.; Science Press: Beijing, China, 2013; pp. 10–19.
19. Oldham, T.R.; McLean, F.B. Total ionizing dose effects in MOS oxides and devices. *IEEE Trans. Nucl. Sci.* **2003**, *50*, 483–499. [CrossRef]
20. *ASTM F996-11*; Standard Test Method for Separating an Ionizing Radiation-Induced MOSFET Threshold Voltage Shift Into Components Due to Oxide Trapped Holes and Interface States Using the Subthreshold Current-Voltage Characteristics. ASTM International: West Conshohocken, PA, USA, 2011. [CrossRef]
21. He, Y.; Shi, Q.; Li, B.; Luo, H.; Lin, L. Oxide-trap and Interface-trap Charge Separation Analysis Techniques on MOSFET. *Reliab. Environ. Test. Electron. Prod.* **2006**, *24*, 26–29. [CrossRef]
22. Wu, H.; Huang, W. A 60V Radiation Hardened VDMOS Power Device. *Reliab. Environ. Test. Electron. Prod.* **2021**, *39*, 33–37.
23. Fan, P. Research on the Radiation and Thermal Stress Reliability of Typical Domestic VDMOS for Satellites Application. Master's Thesis, Shanghai Jiao Tong University, Shanghai, China, 2018.
24. Yang, G.; Wu, W.; Zhang, X.; Tang, P.; Yang, J.; Zhang, L.; Liu, S.; Sun, W. Experimental investigation on total-ionizing-dose radiation effects on the electrical properties of SOI-LIGBT. *Solid-State Electron.* **2021**, *175*, 107952. [CrossRef]
25. Liu, S.; DiCienzo, C.; Bliss, M.; Zafrani, M.; Boden, M.; Titus, J.L. Analysis of Commercial Trench Power MOSFETs' Responses to Co60 Irradiation. *IEEE Trans. Nucl. Sci.* **2008**, *55*, 3231–3236. [CrossRef]
26. Liu, Y.; Chen, H.; He, Y.; Wang, X.; Yue, L.; En, Y.; Liu, M. Radiation effects on the low frequency noise in partially depleted silicon on insulator transistors. *Acta Phys. Sin.* **2015**, *64*, 078501. [CrossRef]
27. Huang, J. Research on Current Model Induced by Total Dose Effects in NMOS Transistors. Master's Thesis, University of Electronic Science and Technology of China, Chendu, China, 2016.

28. Bonaldo, S.; Zhang, E.X.; Zhao, S.E.; Putcha, V.; Parvais, B.; Linten, D.; Gerardin, S.; Paccagnella, A.; Reed, R.A.; Schrimpf, R.D.; et al. Total-Ionizing-Dose Effects in InGaAs MOSFETs With High-k Gate Dielectrics and InP Substrates. *IEEE Trans. Nucl. Sci.* **2020**, *67*, 1312–1319. [CrossRef]
29. Liu, G.Z.; Li, B.; Xiao, Z.Q.; Sun, J.H.; Yu, Z.G.; Wei, J.H.; Wang, H.B.; Hong, G.S.; Shi, J.W. The TID Characteristics of a Radiation Hardened Sense-Switch pFLASH Cell. *IEEE Trans. Device Mater. Reliab.* **2020**, *20*, 358–365. [CrossRef]
30. Shi, M.; Wu, G.; Geng, L.; Zhang, R. *Semiconductor Device Physics*, 3rd ed.; Xi'an Jiaotong University Press: Xi'an, China, 2008; pp. 240–241.
31. Galloway, K.F.; Gaitan, M.; Russell, T.J. A Simple Model for Separating Interface and Oxide Charge Effects in MOS Device Characteristics. *IEEE Trans. Nucl. Sci.* **1984**, *31*, 1497–1501. [CrossRef]
32. Zheng, S.; Zeng, Y.; Chen, Z. Investigation of Total-Ionizing Dose Effects on the Two-Dimensional Transition Metal Dichalcogenide Field-Effect Transistors. *IEEE Access* **2019**, *7*, 79989–79996. [CrossRef]
33. Soliman, F.A.S.; Al-Kabbani, A.S.S.; Rageh, M.S.I.; Sharshar, K.A.A. Effects of electron-hole generation, transport and trapping in MOSFETs due to γ-ray exposure. *Appl. Radiat. Isot.* **1995**, *46*, 1337–1343. [CrossRef]
34. Xie, T.T.; Ge, H.; Lv, Y.H.; Chen, J. The impact of total ionizing dose on RF performance of 130 nm PD SOI I/O nMOSFETs. *Microelectron. Reliab.* **2021**, *116*, 114001. [CrossRef]
35. Sun, Y.B.; Wan, X.; Liu, Z.Y.; Jin, H.; Yan, J.Z.; Li, X.J.; Shi, Y.L. Investigation of total ionizing dose effects in 4H-SiC power MOSFET under gamma ray radiation. *Radiat. Phys. Chem.* **2022**, *197*, 110219. [CrossRef]

Disclaimer/Publisher's Note: The statements, opinions and data contained in all publications are solely those of the individual author(s) and contributor(s) and not of MDPI and/or the editor(s). MDPI and/or the editor(s) disclaim responsibility for any injury to people or property resulting from any ideas, methods, instructions or products referred to in the content.